SLAC-PUB-16162

Exclusive Processes and the Fundamental Structure of Hadrons

Stanley J. Brodsky[1]
[1]*SLAC National Accelerator Laboratory*
Stanford University, Stanford, California 94309, USA

Contribution to the book, '50 Years of Quarks', to be published by World Scientific.

I review the historical development of QCD predictions for exclusive hadronic processes, beginning with constituent counting rules and the quark interchange mechanism, phenomena which gave early validation for the quark structure of hadrons. The subsequent development of pQCD factorization theorems for hard exclusive amplitudes and the development of evolution equations for the hadron distribution amplitudes provided a rigorous framework for calculating hadronic form factors and hard scattering exclusive scattering processes at high momentum transfer. I also give a brief introduction to the field of "light-front holography" and the insights it brings to quark confinement, the behavior of the QCD coupling in the nonperturbative domain, as well as hadron spectroscopy and the dynamics of exclusive processes.

I. INTRODUCTION

One of the most important arenas for testing quantum chromodynamics are measurements of exclusive scattering reactions in which the kinematics of all of the initial and final-state particles are determined. Exclusive processes include hadronic spacelike and timelike hadronic form factors, two-photon reactions $\gamma\gamma \to H\bar{H}$, Compton scattering $\gamma p \to \gamma p$, deeply virtual Compton scattering $\gamma^* p \to \gamma p$; and two-body scattering reactions such as elastic proton-proton scatting $pp \to pp$ and pion photoproduction $\gamma^* p \to \pi^+ n$. In such reactions one is sensitive to the fundamental composition of hadrons in terms of their quark and gluon content, as well as the fundamental interactions and forces acting on their quark and gluonic constituents. Exclusive reactions are also sensitive to the dynamics of color confinement, and they illuminate the mechanisms underlying quark and gluon hadronization at the amplitude level in quantum chromodynamics (QCD).

A central feature of exclusive processes are the *"constituent counting rules"* which allow one to verify the underlying quark and gluon content of hadrons and enumerate their fundamental degrees of freedom. The counting rules were derived in the 1970's by Farrar and this author [1, 2] and by Matveev, Muradyan and Tavkhelidze [3], soon after the development of QCD by Fritzsch, Gell Mann, and Leutwyler [4]

This review begins with a summary of the main features of quark counting rules and quark interchange phenomena– which gave early validation of the quark structure of hadrons. I then review the development of perturbative QCD factorization theorems and the evolution equations for the hadron *"distribution amplitudes* – the fundamental wavefunctions which control form factors at large momentum transfer and other hard scattering exclusive scattering processes. I also give a short introduction to"light-front holography" and the insights it brings to quark confinement, the QCD coupling in the nonperturbative domain, light-quark hadron spectroscopy, and the dynamics of exclusive processes.

II. QUARK COUNTING RULES

The physics principle underlying the counting rules is that at momentum transfers large compared to the QCD color confinement scale, where asymptotic freedom is applicable, the dominant internal interactions between quarks from gluon exchange within hadrons should be approximately scale independent. in fact, close to conformal [5, 6]. The twist-dimension of the effective operator which creates the hadron at short distances [7, 8] then controls the scaling of an exclusive amplitude. Here 'twist' refers to the dimension minus the spin of the interpolating operator; it also

This material is based upon work supported by the U.S. Department of Energy, Office of Science, Office of Basic Energy Sciences, under Contract No. DE-AC02-76SF00515 and HEP.

equals the number of quarks in the valence Fock state; e.g., the twist is 3 for baryons and the twist is 2 for mesons; higher Fock states will give "higher twist" power-law suppressed contributions. The result is that the power-law fall-off of any hard-scattering reaction can be predicted by simply counting the number of bound quarks in each of the interacting hadrons, thus providing a direct window to their constituent structure. Thus, according to the counting rules, an exclusive scattering amplitude at large momentum transfer such as elastic hadron-hadron scattering at fixed θ_{CM} (or fixed t/s) will have the nominal power-law fall-off[1–3]

$$M(A+B\to C+D)=\frac{F_{A+B\to C+D}(\theta_{CM})}{s^N}$$

where

$$N=n_A+n_B+n_C+n_D-4.$$

Here n_i is the minimum number of fundamental ("valence") constituents in each hadron's wavefunction; e.g., one counts $n_B=3$ for baryons, $n_M=2$ for mesons , and $n=1$ for interacting elementary particles such as the photon or lepton. Thus for any two-to-two scattering process the differential cross section will fall as

$$\frac{d\sigma}{dt}(A+B\to C+D)\propto\frac{|M(A+B\to C+D)|^2}{s^2}\propto\frac{|F_{A+B\to C+D}(\theta_{CM})|^2}{s^{2N-2}}$$

at large center-of mass energy squared $s=E_{CM}^2$ and fixed ratio of invariants such as fixed t/s or fixed center-of mass angle θ_{CM}. A simple example is meson-baryon photoproduction:

$$\frac{d\sigma}{dt}(\gamma p\to K^+\Lambda)\propto\frac{|F(\theta_{CM}|^2}{s^7}$$

since $N=3+1+2+3-2=7$.. The experimental test of the counting rule for proton-proton elastic scattering at fixed θ_{CM} is shown in fig. 1. The quark counting prediction is $N=12-2=10$, and the best fit to the data is $N=9.7\pm0.5$ [9]

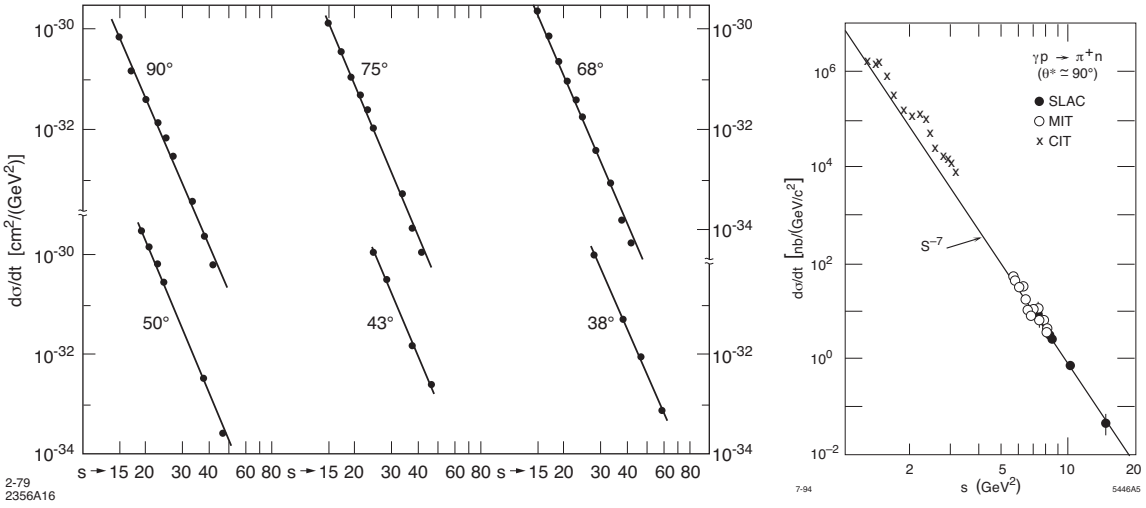

FIG. 1: Data for $\frac{d\sigma}{dt}(pp\to pp)$ and $\frac{d\sigma}{dt}(\gamma p\to\pi^0 p)$ The measured power-law fall-off at fixed θ_{CM} are consistent with the quark counting rule predictions s^{-10} and s^{-7}, respectively. Further details and references can be found in [10].

In general one finds that the fall-off predicted by quark counting is consistent with measurements when the momentum transfer p_T in the hard exclusive reaction exceeds a few GeV. Here $p_T^2=tu/s$. The counting rule for elastic lepton-hadron scattering $\ell H\to\ell H$ also predicts the power-law fall-off of the dominant helicity-conserving hadron's form factor at large $Q^2=-t$:

$$F_H(Q^2)\propto[1/Q^2]^{n_H-1},$$

where n_H is the minimum number of elementary constituents in H; i.e. the 'twist' of the leading interpolating operator of the hadron H at small distances. Thus meson form factors fall-off as $1/Q^2$, the Dirac form factor falls at $1/Q^4$. A

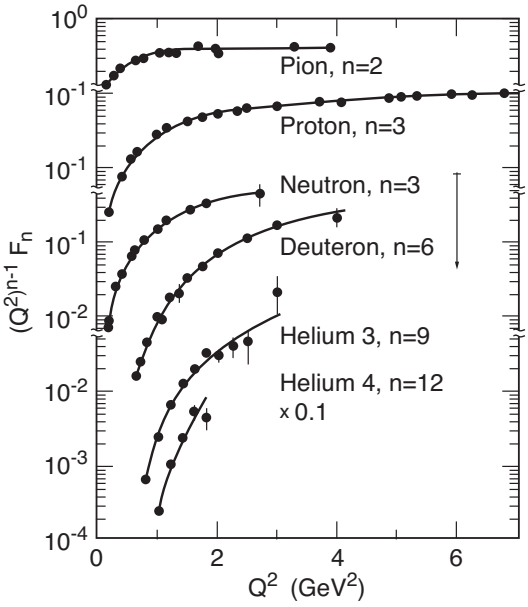

FIG. 2: Tests of quark counting for meson, nucleon and nuclear form factors at high momentum transfer : $[Q^2]^{n_H-1} \times F_H(Q^2) \rightarrow$ constant. Further details and references can be found in [11]

comparison with data is given in fig. 2. Historically, the empirical success of the counting rules provided a primary check on the number of valence quarks underlying the bound-state structure of hadrons. Furthermore, they provided a test on the elementary, structureless property of photons, leptons, as well as the intermediate bosons exchanged in charged- or neutral-current exclusive processes. The counting rules can also be applied to large-angle real or virtual Compton scattering, hard exclusive nuclear reactions such as $\gamma d \rightarrow np$. They can also be extended to exclusive processes involving the production of multiple hadrons, such as $p\bar{p} \rightarrow K^+K^-\pi^0$. A detailed review is given in ref. [11]

Because of the Drell-Yan exclusive-inclusive connection [12], the quark counting rules for form factors at large momentum transfer also imply counting rules for the power-law falloff of the quark and gluon structure functions in hadrons : $G_{a/H}(x)$ at $x \rightarrow 1$, the kinematic domain where the constituent a takes most of the momentum of the hadron H. The limiting power-law behavior at $x \sim 1$ of the distributions derived from minimally connected amplitudes is [13]

$$G_{a/H}(x) \propto (1-x)^p$$

where

$$p = 2n - 1 + 2\Delta S_z$$

Here n is the minimal number of spectator quark lines, and $\Delta S^z = IS_a - S_H|$. For example $\Delta S^z I = 0 or 1$ for parallel or anti-parallel quark and proton helicities, respectively. This counting rule reflects the fact that the valence Fock states with the minimum number of constituents give the leading contribution to structure functions when one quark carries nearly all of the light-cone momentum. Thus Fock states with a higher number of partons give structure functions which fall off faster at x 1. The helicity dependence of the counting rule also reflects the helicity retention properties of the gauge couplings: a quark with a large momentum fraction of the hadron also tends to carry its helicity; the anti-parallel helicity quark is suppressed by an extra suppression of $(1-x)^2$. The counting rule for valence quarks can be combined with the splitting functions to predict the $x \sim 1$ behavior of gluon and non-valence quark distributions. In particular, the gluon distribution of non-exotic hadrons must fall by at least one power faster than the respective quark distributions. The counting rules for large x behavior of quark and gluon helicity distributions can also be derived from the continuity between the exclusive and inclusive channels at fixed invariant mass. For example, as shown by Drell and Yan [12], a quark structure function $G_{q/H} \sim (1-x)^{2n-1}$ at $x \rightarrow 1$ if the corresponding form factor $F(Q^2) \propto (1/Q^2)^n$ at large Q^2. A similar analysis controls the $z \rightarrow 1$ behavior of the fragmentation functions $D_{H/a}(z)$. The results are constant with Gribov-Lipatov crossing relations. Higher twist corrections due to multiparton subprocesses are discussed in ref. [14]

The quark counting rules were later shown to explicitly emerge from pQCD factorization theorems by Brodsky and Lepage [15, 16] and by Efremov and Radyushkin [17]. As we shall review below, one also predicts logarithmic

corrections to the nominal power law fall-off which can be systematically derived from two sources: the evolution of the QCD coupling constant $\alpha_s(Q^2)$ and the evolution of the hadron distribution amplitudes, the fundamental gauge-invariant amplitudes which control hadronic process at short distances. More recently, the quark counting rules were shown [18] to be features of a nonperturbative approach based on AdS/QCD and light-front holography, the postulated duality between AdS_5 space and QCD in physical space-time. This analysis is discussed further in section VI.

The pQCD analysis also predicts a number of other phenomenological features of hard exclusive processes. These include

- **Hadron Helicity Conservation** [19]The dominant pQCD interactions conserve quark chirality at every quark vertex such as $gq_\uparrow \to q_\uparrow$ and $g \to q_\uparrow \bar{q}_\downarrow$. The quark-chirality interactions bring in powers of the quark mass and thus faster power fall-off. in addition, the leading power contribution to hard exclusive amplitudes are derived from wavefunctions with zero quark orbital angular momentum. Thus the total S^z of the incident and final hadrons is conserved at leading twist :

  $$\lambda_A + \lambda_B = \lambda_C + \lambda_D.$$

  This rule also accounts for the dominance of helicity-conserving form factors, such as the dominance of the Dirac hadron helicity-conserving form factor of the proton $F_1(Q^2) \propto \frac{1}{Q^4}$ relative to the helicity-flip Pauli form factor $F_2(Q^2) \propto \frac{1}{Q^6}$ at a high momentum transfer $Q^2 = -t >> \Lambda^2_{QCD}$. However, the dominant decay $J/\psi \to \pi\rho$ violates hadronic helicity conservation as well as the OZI rule. The solution [20] to this anomaly may be connected to higher Fock states of the final-state mesons which contain "intrinsic " $c\bar{c}$ pairs. A discussion of this puzzle is given in ref. [21]

- **Color Transparency** [22–24] Perturbative QCD predicts that at high moment transfer $p_T^2 >> \Lambda^2_{QCD}$, the hadronic wavefunctions which control hard scattering amplitudes are dominated by configurations where all of the hadron constituents have small impact separation $\frac{b_\perp 1}{p_T^2}$. These configurations interact weakly inside a nuclear environment because of their small color-dipole moment; i.e., the color gauge interactions of the quark and antiquark of a meson tend to cancel when they have small impact separation. Thus a hard-scattering exclusive reaction can occur anywhere in the nucleus in a quasielastic reaction such as $pA \to ppX$ without absorption in the initial or final state. These small-size configurations expand to physical size hadrons at a time interval proportional to the hadron's energy. The cross section for $pA \to ppX$ is thus predicted to be additive in the number of protons in the nuclear target at very large momentum transfer: $E\frac{d\sigma}{d^3p}(pA \to ppX) \simeq ZE\frac{d\sigma}{d^3p}(pp \to pp)$ The expectations of color transparency have been verified in hard exclusive channels such as $\gamma^* p \to \rho^0 p$ at high photon virtuality Q^2 and high momentum transfer quasi-elastic pp scattering. Comprehensive reviews are given in ref. [24, 25] The color transparency of hard exclusive reactions is in direct contradiction to traditional Glauber theory [26], where the large size of hadron-nucleon cross sections implies that hadronic interactions in a nuclear target are relegated to the nuclear periphery. For example, in low momentum transfer reactions the cross section $\sigma(pA \to \pi X)$ behaves $A^{1/3}$ since the proton can only interact on the front surface, and thus the emitted pion can only emerge from the nuclear perimeter [27].

  Color transparency was tested directly in the dijet diffractive reaction $\pi A \to JetJetA'$ in a Fermilab experiment by Ashery et al. [25, 28] The emerging jets correspond to the dissociation of the pion $\pi \to q\bar{q}$ with closely balanced transverse momenta $\sim \pm\vec{k}_\perp$, so that the nucleus remains intact. See fig. 3. At large $k_\perp^2$ the dominant configurations of the pion wavefunction have small impact separation $b_\perp^2 \sim 1/k_\perp^2$ and thus small color dipole moments. The measurements of the nuclear A dependence are in agreement with the color transparency predictions of Strikman et al. [25, 28]

  However, In one classic experiment, color transparency was observed to fail dramatically: A strong nuclear suppression is observed in $pA \to ppX$at $\sqrt{s} \simeq 5\ GeV$. [29]; this is the same energy where a surprisingly strong spin-spin correlation $R_{NN} \simeq 4$ is observed [30]. Here R_{NN} is the ratio $\frac{d\sigma}{dt}(p_\uparrow p_\uparrow \to pp)/\frac{d\sigma}{dt}(p_\downarrow p_\downarrow \to pp)$, where the incident protons are polarized normal to the scattering plane. The anomalously strong spin-spin correlation and the associated breakdown of color transparency can be understood as due to the physics of the charm threshold [31]: $\sqrt{s} \simeq 5\ GeV$ is the energy where a produced $c\bar{c}$ plus the six spectator light quarks are all at the same rapidity and thus can interact strongly. In fact, one can interpret the data for evidence for the production of an "octoquark " $|uuduudc\bar{c}>$ resonance in the $J = 1, S = 1$ $pptopp$ partial wave. [21, 31, 32]. Large-size protons are involved, and thus color transparency breaks down in the energy domain where the octoquark resonance is excited.

- **Nuclear Effects and Hidden Color** At first approximation, a nucleus can be regarded a composite of protons and nuclei bound by the exchange of mesons. However, quantum chromodynamics predicts that at high

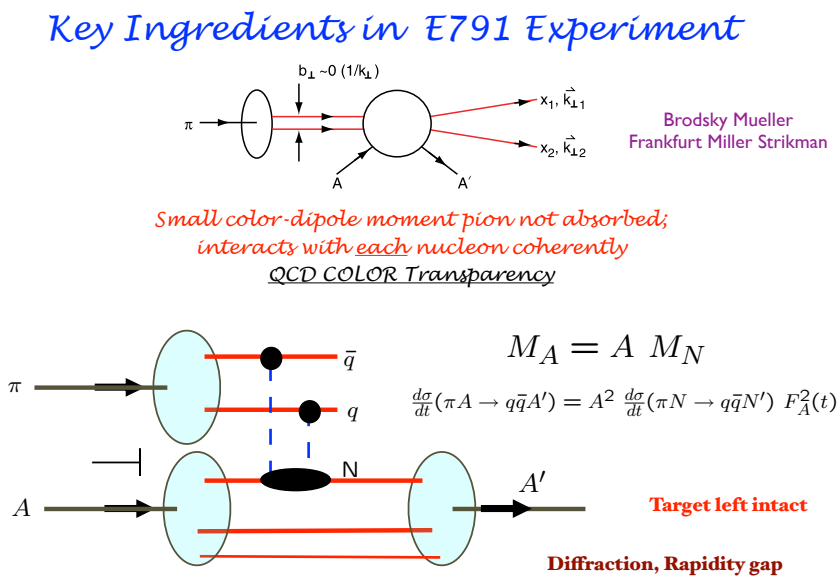

FIG. 3: Illustration of pion diffractive dissociation to dijets in a nucleus $\pi A \to \text{JetJet} + A$. The nucleus A remains intact. When the jets are produced at high and opposite transverse momenta $\pm\vec{p}_\perp$, one samples the pion LF wavefunction at $b_\perp \simeq \frac{1}{p_\perp}$ where the quark and antiquark have small transverse separation; i.e., the dijet has a small color dipole moment. The color transparency prediction of negligible absorption in the nucleus was verified by the FermiLab experiment of Aitala, et al. [25, 28]

resolution, the structure of the nucleus is much more complex: the nucleus itself becomes revealed as a bound-state system of confined quarks and gluons, the fundamental quantum fields of QCD. Even the fundamental nature of the nuclear force is reinterpreted in QCD. In fact, measurements of the elastic scattering of protons at high momentum transfer show that the dominant interaction at short distances between nucleons is the interchange of their constituent quarks [33].

An important example where QCD differs from traditional nuclear physics in a fundamental way is presence of the "hidden-color" degrees of freedom in the nuclear eigensolution [34–37] If one regards the deuteron as a composite of six color-triplet quarks, then there are five different color-singlet states, only one of which matches the usual proton-neutron degrees of freedom. In fact, when one considers color-octet gluon exchange at short inter-nucleon distances, then all five color-singlet components enter the deuteron eigensolution. This can be shown explicitly using rigorous pQCD evolution equations which couple together all of the components [38] One can prove from the evolution of the deuteron distribution amplitude [38] that at $Q^2 \to \infty$ all five color-singlet components have equal weight.

Thus QCD predicts the dominance of the hidden-color configurations when a deuteron scatters at very large momentum transfers in elastic electron-deuteron scattering, or when it photo-disintegrates into pairs of baryonic resonances, or when the quark in the nucleus carries a high momentum fraction $x > 1$, beyond the kinematics of a single nucleon. The hidden-color degrees of freedom can manifest themselves as the dominant contribution to the elastic form factor of the deuteron at very large Q^2. It is useful to factorize the deuteron helicity-conserving form factor $F_d(Q^2) = A(Q^2)$ in the form [34]

$$F_d(Q^2) \equiv F_p(Q^2/4)F_n(Q^2/4)F_d^{reduced}(Q^2)$$

since in the weak binding limit each nucleon scatters in electron-deuteron elastic scattering with half the momentum transfer. The quark counting rules predict $F_d^{reduced}(Q^2) \sim \frac{1}{Q^2}$, the same scaling as a meson. This scaling prediction has been confirmed experimentally [35] See fig. 4. The magnitude of $Q^2 F_d^{reduced}(Q^2)$ is much larger than expected from conventional nuclear physics based on the small deuteron binding, thus indicating a dominant role of hidden color in the hard-scattering domain'[38]. The hidden color of the deuteron LFWF also predicts a large coupling of $\gamma d \to \Delta^+\Delta^0$ in exclusive photodisintegration [39]

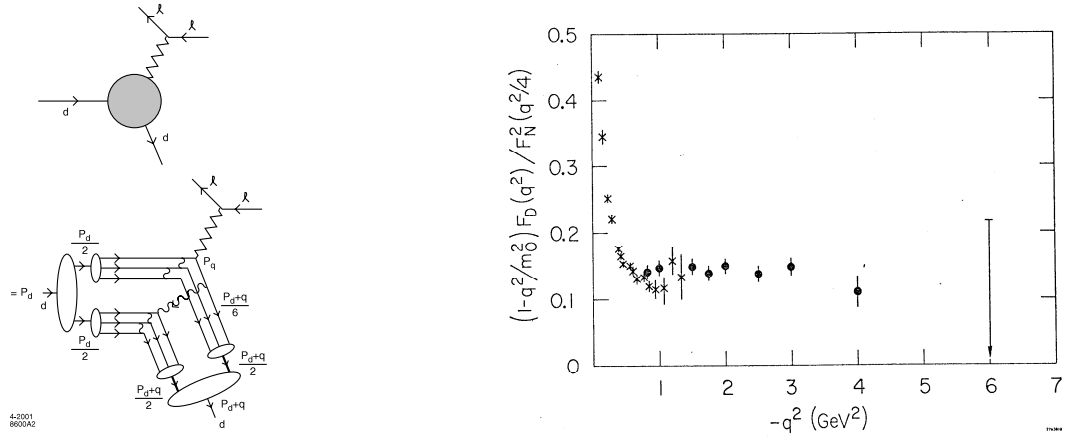

FIG. 4: (a) Physics of of the deuteron reduced form factor $F_d^{reduced}(Q^2)$. In the weak binding limit, each nucleon scatters in electron-deuteron elastic scattering with half the momentum transfer. (b) Experimental test of the scaling prediction $Q^2 F_d(Q^2) \to$ constant for the reduced deuteron form factor.

III. THE FRONT FORM

The light-front (LF) formalism is based on Dirac's "front form" [40], where the time variable $\tau = t + z/c$ is the time along the light-front. For a review, see [41]. For example, when when one takes a flash photograph, the resulting photographs is at fixed light-front time τ. In fact physical measurements such as deep inelastic scattering on a proton capture the structure of the proton at fixed LF time within the causal horizon, not at a fixed "instant" time t which would requires acausal information. The form factors are thus a primary measure of hadron structure at fixed LF time $\tau = t + z/c$. Given the QCD Lagrangian, one can derive the LF Hamiltonian $H_{LF} = -i\partial/\partial\tau$, the LF time evolution operator.

The eigensolutions of the QCD light-front Hamiltonian for each hadron satisfy the LF Heisenberg equation:

$$H_{LF}|\Psi_I >= M_I^2|\Psi_I >$$

where the eigensolution $\Psi_H >$ for each hadron H can be expanded as a sum over free Fock states:

$$|\Psi_H >= \sum_n \psi_n/H(x_i, \vec{k}_{\perp_i}, \lambda_i)|n >$$

The n constituents of the Fock states $|n >$ for a hadron with momentum $P^{\pm} = P^0 \pm P_z$ and $\vec{P}_\perp$ have physical momenta $p_i^+ = x_i P^+$ and $\vec{p}_{\perp i} = x_i \vec{P}_\perp + \vec{k}_\perp >$. The momenta $k^+ = k^0 + k^z$ are conserved and always positive. One also has $M^2 = P^+P^- - P_\perp^2$. The Fock state with minimum n (n=2 for mesons and n=3 for baryons) are called the "valence" Fock states. Since the + and transverse momenta are conserved in the front form, $\sum_i^n x_{i-1} = 1$ and $\sum_i^n \vec{k}_{\perp_i} = 0$.

The coefficients in the Fock expansion are the hadronic light-front wavefunctions. See fig. 5. The LFWFs are the hadronic eigensolutions of H_{LF} which in turn is derived from the QCD Lagrangian. They control virtually every observable in QCD. See fig.6. A remarkable feature of the light-front formalism is that the LFWFs are independent of the hadron's momentum P^+ and $P_\perp$. No Wigner or Melosh boosts are required. In principle, the LF Heisenberg equation can be solved by matrix diagonalization of the LF Hamiltonian using discretized light-cone quantization (DLCQ). [41–44] In fact this can be done to essentially arbitrary accuracy for QCD [45] and other theories [46] in one space and one LF time. As we shall discuss in section VI, one can obtain predictions for the nonperturbative LFWFs of hadrons with confined quarks from a novel method called "light-front holography" [47].

Form factors and other current matrix elements $< p+q|J^\mu(0)|p >$ which are measured by virtual photon exchange in elastic or inelastic lepton-hadron scattering can be elegantly written in terms of the overlap of initial-state and final-state light-front wavefunctions (LFWFs) of the hadrons [12, 48, 49]. The Drell-Yan-West (DYW) formula [12, 48, 49] for the spacelike ($t < 0$) form factor of a spin-zero meson form factors is given by the overlap of initial and final-state light-front wavefunctions:

$$F(q^2) = \int d^2\vec{k}_\perp \int_0^1 dx \psi_H(x, \vec{k}_\perp)\psi_H(x, \vec{k}_\perp + (1-x)\vec{q}_\perp)$$

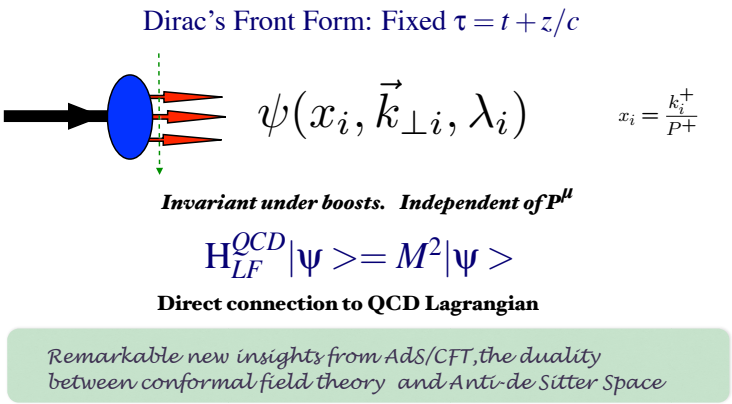

FIG. 5: Light-Front wavefunctions are the frame-independent hadronic eigensolutions of the light-front Hamiltonian H_{LF}, which in turn is derived from the QCD Lagrangian.

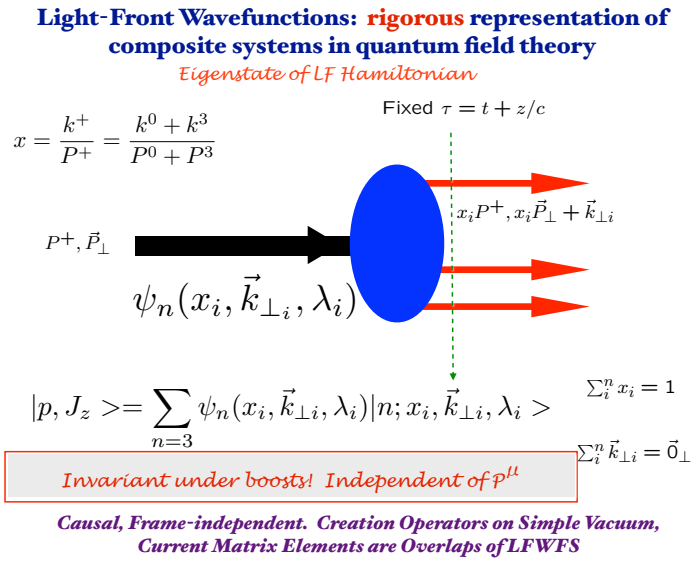

FIG. 6: The LFWF describes the state at a fixed LF time $\tau = t + z/c$ and is off-shell in $P^- = \frac{\mathcal{M}^2 + P_\perp^2}{P^+}$ and thus in invariant mass. The Fock state wavefunctions $\psi_n(x_i, \vec{k}_{\perp i}, \lambda_i)$ are independent of the hadron's 4-momentum $P^\mu = (P^+, P^-, \vec{P}_\perp)$. The LFWFs can also be predicted from light-front holography.

where $t = -q^2 < 0$. (A sum over the struck quarks weighted by the quark charge and a sum over all hadronic Fock states is understood.). An essential step in the derivation of the DYW formula is to evaluate the current matrix element $F(q^2) = < p + q|j^+(0)|p > /P^+$ in the Lorentz frame with $q^+ = 0$ and thus $-t = -q^2 = Q^2 = \vec{q}_\perp^2$. Thus the kinematical coordinates of the exchanged virtual photon is $q^\mu = (q^+, q^-, \vec{q}_\perp) = (0, q^-, q_\perp)$, where $q_\perp^2 = Q^2 = -q^2$ and $q^- = 2p \cdot q/P^+$. The choice $q^+ = 0$ avoids the need to evaluate contribution from the overlap of LFWFs with different number of constituents. Since $q^+ = 0$, LF coordinate $x = k^+/P^+$ does not change at the quark-photon-quark vertex. See fig. 7.

If the struck quark of the initial state has LF momenta $k_\perp$ and x, then the momenta of the final-state constituents are x and $k_\perp + (1 - x)\vec{q}_\perp$ for the struck quark and x and $\vec{k}_{\perp I} + x_i \vec{q}_\perp$ for the spectator constituents. In the case of

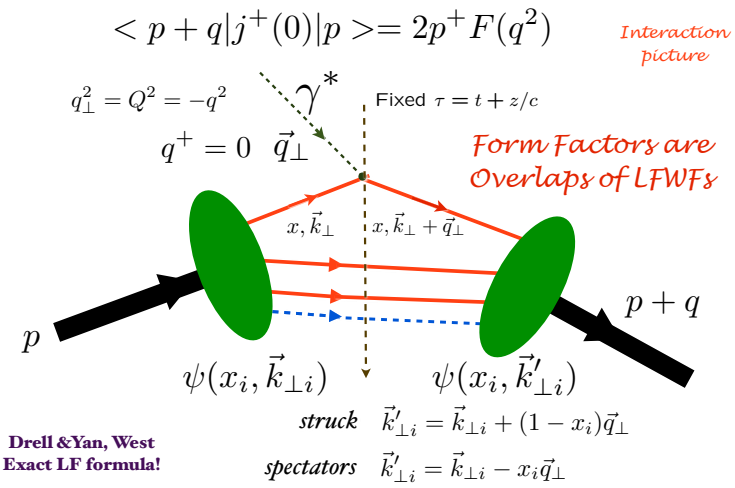

FIG. 7: Illustration of the Drell-Yan West formula for the calculation of form factors and other current matrix elements as overlaps of boost-invariant LFWFs.

spin, the LFWFs multiply LF spinors where $\bar{u}\gamma^+ u = 1$. Thus the DYW LF formula holds for the Dirac form factor $F_1(q^2)$ where the initial and final state nucleon have the same helicity. The corresponding formula for the spin-flip Pauli form factor $F_2(q^2)$ is: [49]

$$(\vec{q}_\perp x + i\vec{q}_\perp y) \times F_2(q^2) = < p+q, S^z = -1/2|j^+(0)|p, S^z = +1/2 > /P^+$$

$$= \int d^2\vec{k}_\perp \int_0^1 dx \psi_H^{S_z=-1/2}(x, \vec{k}_\perp)\psi_H^{S^z=1/2}(x, \vec{k}_\perp + (1-x)\vec{q}_\perp)$$

Since the quark spin is not flipped by the current operator j^+, the Pauli form factor is the overlap of the initial-state LFWF where the spin of struck quark is parallel to the proton spin with the spin-antiparallel LFWF of the final state baryon. Thus the quarks in the baryon must have orbital angular momentum in order to have a nonzero Pauli form factor and nonzero anomalous moment. These frame-independent light-front expressions are the relativistic generalizations of the overlap formula of Schrödinger wavefunctions for form factors in nonrelativistic quantum mechanics. One can immediately derive the quark counting rules for form factors by noting that the LFWFs fall-off as $\frac{1}{k_\perp^2}$ at large $k_\perp$ for each pair of internal interactions.

The simplicity of the DYW formula for current matrix elements is remarkable. One can also derive an exact formula in the two-particle Bethe-Salpeter formalism by integrating first over k^-. In fact, the LFWFs are related to the Bethe Salpeter wavefunctions evaluated at fixed LF time τ [50]. However, all cross-graph kernels must appear in the BS formalism in order to maintain crossing symmetry. In fact, one must include all crossed-graph kernels simply to recover the familiar Dirac-Coulomb equation and the form factors of the muonium μ^+e^- atom at infinite muon mass [51].

If one tries to evaluate form factors using "instant" time, one must include contributions where the virtual photon interacts with the connected currents from $q\bar{q}g$ vertices appearing from the vacuum. One must also boost the instant-form wavefunctions [52], a formidable dynamical problem and also include the overlaps of Fock states with different particle number. The instant form expressions are frame-dependent and acausal. One can formally recover the DYW formula in the instant form by evaluating the current matrix element in a Lorentz frame with $P^z \to -\infty$, the "infinite momentum frame" [53, 54]. However, it is much more natural to simply quantize at fixed τ.

As discussed by Soper [55], the exact DYW expression for form factors and other current matrix elements can be written in coordinate space:

$$F(q^2) = \int_0^1 dx \int d^2\vec{\eta}_\perp e^{i\vec{\eta}_\perp \cdot \vec{q}_\perp} \tilde{\rho}(x, \vec{\eta}_\perp)$$

where x is the LF momentum of the struck quark, $q_\perp^2 = Q^2$ and $\vec{\eta}_\perp = \sum_{j=1}^{n-1} x_j \vec{b}_\perp$. For example, in the case of the valence $q\bar{q}$ Fock state of a meson , $\vec{\eta}_\perp = (1-x)\vec{b}_\perp$, where $\vec{b}_\perp$ is the transverse impact coordinate conjugate to $-\vec{k}_\perp$. At large $Q^2 = -q^2$, $F(q^2)$ is dominated by the LF density $\tilde{\rho}(x, \vec{\eta}_\perp)$ in the domain $\vec{\eta}_\perp^2 =< \frac{1}{Q^2}$. This condition is true for all Fock states, independent of the number of constituents. The small $\vec{\eta}_\perp^2$ domain corresponds to small frame-independent separation of the constituents of the hadron; only small color dipole moments then appear– the underlying physics for color transparency. The region of fixed $k_\perp$ at $x \simeq 1$ has no special role.

IV. DOMINANCE OF QUARK INTERCHANGE

One of the prominent features of atom-atom scattering in QED is the dominance of electron exchange [56]: two atoms can scatter by exchanging an electron. This process is called 'spin-exchange' since the spins of the exchanged electrons can be interchanged. The interchange amplitude is the physics underlying the covalent bond when the two atoms form a molecule. The analog of electron interchange in atom-atom scattering is quark interchange [33]. For example, in $K^+p \to K^+p$ elastic scattering, the u quark common to both hadrons can be exchanged. This is illustrated in fig. 8. The interchange amplitude can be expressed as a simple overlap of the four light-front wavefunctions of the

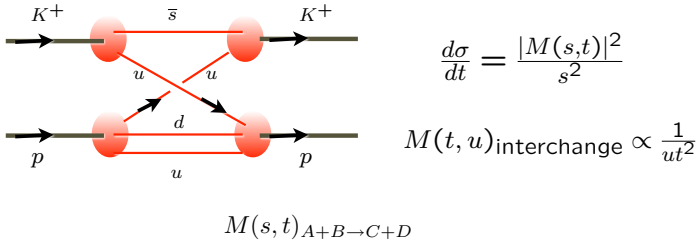

FIG. 8: The quark interchange mechanism for K^+p elastic scattering.

interacting hadrons [33]:

$$M^{AB\to CD}_{interchange}(s,t) = \frac{1}{2(2\pi)^3}\int d^2\vec{k}_\perp \int_0^1 dx \psi_A(x, \vec{k}_\perp + (1-x)\vec{q}_\perp + x r_\perp)\psi_C(x, \vec{k}_\perp + x\vec{r}_\perp)\times$$

$$\Delta(x, \vec{k}_\perp) \times \psi_B(x, \vec{k}_\perp)\psi_D(x, \vec{k}_\perp + (1-x)\vec{q}_\perp)$$

The kinematics require $q_\perp^2 = -t$, $\vec{r}_\perp^2 = u$ and $\vec{r}_\perp \cdot \vec{q}_\perp = 0$. The Mandelstam variables satisfy $s + t + u = \sum_i M_i^2$. The quantity $\Delta = \sum_{I=A,B,C,D}(s - K_a - K_b - K - c - K_d$ is the inverse of the LF energy denominator which appears during the interchange of the quarks, where $K_i = (k_{\perp i}^2 + m_i^2)/x_i$, $(i = a, b, c, d)$ is the LF kinetic energy of each constituent in that intermediate state. The quantity Δ is in effect the sum of the internal binding potentials $\sum_{i=1}^4 V_i$ summed over the four hadrons. The resulting differential cross section is then

$$\frac{d\sigma}{dt}(AB \to CD)(s,t) = \frac{1}{s^2}|M^{AB\to CD}_{interchange}(s,t)|^2$$

This relativistic amplitude reduces in the nonrelativistic limit to an overlap of Schrodinger wavefunctions.

The interchange amplitude can also be written in impact space in a form similar to that of the Soper equation, where now the exponential involves $\vec{\eta}_\perp \cdot \vec{q}_\perp$ and $\vec{\eta}_\perp \cdot \vec{r}_\perp$. Since they are orthogonal vectors, we can take $\vec{r}_\perp \propto \hat{x}$ and $\vec{q}_\perp \propto \hat{y}$ In this case the hard-scattering domain of high u and high t (or high $p_t^2 = tu/s$ and fixed θ_{CM}) requires the LF density $\tilde{\rho}$ to be evaluated at $\vec{\eta}_y^2 =< \frac{1}{|t|}$ and $\vec{\eta}_x^2 =< \frac{1}{|u|}$. This establishes the short-distance dominance and color transparency of the amplitude. The quark counting rules also emerge. (The argument works in 3+1 space because there are two transverse directions. It would not work for $A + B \to C + D + E$ at fixed angle!) In the case of $K^+p \to K^+p$ elastic scattering, the quark constituent interchange prediction is

$$M_{CIM}^{K^+p\to K^+p}(s,t) \propto \frac{\kappa^6}{ut^2}$$

at high u and t; it agrees well with measurements. See Fig. 9. Here κ represents the mass scale of QCD. The $1/u$ dependence of the amplitude extends Regge theory to the large spacelike momentum transfer; in fact, the Regge trajectory curves over to $\alpha_R(t) \to -1$ at large t; it is no longer linear. The corresponding interchange amplitude for nucleon-nucleon elastic scattering is

$$M_{CIM}^{p+p\to p+p}(s,t) \propto \frac{\kappa^8}{u^2t^2}$$

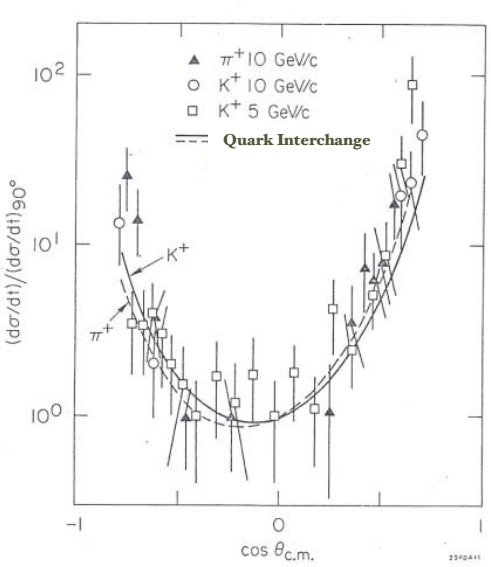

AdS/CFT explains why quark interchange is dominant interaction at high momentum transfer in exclusive reactions

$M(t,u)_{\text{interchange}} \propto \frac{1}{ut^2}$

Non-linear Regge behavior:

$\alpha_R(t) \to -1$

FIG. 9: Data for $K^+p \to K^+p$ elastic scattering at fixed θ_{CM}. The data are consistent with the $u-$quark interchange prediction $M_{K^+p\to K^+p} \propto 1/ut^2$, Reggeon intercept $\alpha_R(t) \to -1$ at large t, and the $1/s^8$ scaling of the cross section.

One of the striking features of hard two-body exclusive hadronic scattering reactions is the strong dominance of the quark exchange or interchange contributions over gluon exchange. In fact, White et al. [57] have analyzed 20 different exclusive processes and found that the quark exchange amplitude strongly dominates over gluon exchange in every reaction. This is particularly surprising since Landshoff [58] has shown that the amplitude where three gluons – each exchanging one-third of the momentum transfer between each quark-quark pair – should strongly dominate in large-angle hard $pp \to pp$ elastic scattering if one compares amplitudes. See also ref. [1, 59]. However, there is no sign of the expected gluon-exchange contribution in the measured cross section. The strong dominance of the interchange amplitude may be due to the fact that no extra interactions are needed beyond the internal dynamics of confinement when one evaluates the quark interchange amplitude; all of the effects of gluon exchange at the small $t/9$ virtualities involved in these elastic scattering reactions may be encapsulated as a 'flux tube' [60] which generates the color confinement potential. If this is the case, hard gluon interactions may become manifest at very large momentum transfers. Other examples where gluon exchange contributions are evidently absent and the OZI rule fails are discussed in ref. [21]

V. PERTURBATIVE QCD FACTORIZATION FOR HARD EXCLUSIVE PROCESSES

One of fundamental testing grounds for perturbative QCD are hard exclusive processes. Rigorous theorems based on factorization of the hard and soft dynamics and the operator product expansion (OPE) can be based on first principles in QCD. An introduction to the theory of exclusive reactions and additional references are given in ref. [11]. For a recent review and applications to deeply virtual Compton scattering, see ref.[59].

At high momentum transfer large compared to the QCD nonperturbative scale, hadronic amplitudes can be factorized at leading power as a convolution [16, 17] of a hard scattering amplitude T_H with the product of process-independent hadronic distribution amplitudes $\phi_H(x_i, Q)$. The hard-scattering amplitude T_H is obtained by replacing each hadron by its valence quarks, moving as free partons collinear with the hadron. For example, for meson-meson scattering the factorization takes the form

$$\mathcal{M}_{A+B\to C+D} = \int dx_i \phi_C(x_c, \lambda_c, \tilde{Q}) \phi_D(x_d, \lambda_d, \tilde{Q}) T_H(x_i, \lambda_i, Q^2, \theta_{cm}) \times \phi_A(x_a, \lambda_a, \tilde{Q}) \phi_B(x_b, \lambda_b, \tilde{Q})$$

where the x_i are the light-front fractions $x_i = k_i^+/P_H^+$ carried by each valence quark in the initial-state and final-state hadrons, and the $\lambda_i = S_i^z = \pm 1/2$ are the respective LF spin projections of the quarks. The distribution amplitude $\phi_H(x, \tilde{Q})$ defined below is the interpolating amplitude between the valence quarks and the full dynamics of the hadron. The pQCD factorization is illustrated for meson-baryon elastic scattering in fig. 10 and for the proton form factor

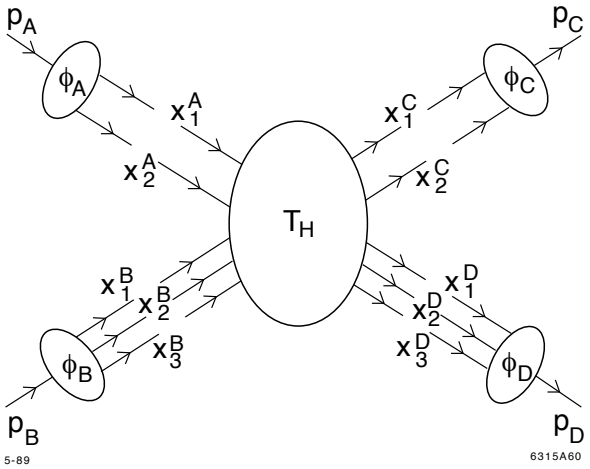

FIG. 10: PQCD factorization of the hard scattering amplitude for elastic meson-baryon scattering at large momentum transfer.

(

in fig. 11. In the case of two-photon annihilation into meson pairs the incident photons act as elementary fields at leading order in $1/p_T$. One then has

$$\mathcal{M}_{\gamma\gamma\to M\bar{M}} = \int_0^1 dx \int_0^1 dy \phi_{\bar{M}}(y, \tilde{Q}_y) T_H(x, y, s, \theta_{cm}) \phi_M(x, \tilde{Q}_x)$$

where T_H is the scattering amplitude for $\gamma\gamma \to [q\bar{q}][q\bar{q}]$ computed as if each valence quark and anti-quark is collinear to the momentum of its respective ingoing or outgoing meson. Here $\tilde{Q}_x = min_{x_1,x_2} Q$. PQCD factorization can also be applied to obtain the leading contribution to hard exclusive scattering amplitudes such as Compton scattering, exclusive two-photon annihilation amplitudes, meson photoproduction, and baryon-baryon scattering, as well as deeply virtual Compton scattering $\gamma^* p \to \gamma p$. In each case, the hard-scattering amplitude T_H can be computed order by order in pQCD, starting with the sum of Born diagrams at first order $\alpha_s(p_T^2)$ connected by a single exchanged gluon.

The gauge invariant hadron distribution amplitudes $\phi_H(x_i, Q)$ contain the fundamental nonperturbative dynamics of QCD in the short distance regime [61]. The distribution amplitude in light-cone gauge is the integral over transverse momentum of the hadron LFWF $\psi_H(x_i, k_{\perp i})$, the valence Fock state eigensolution of the QCD light-front Hamiltonian:

$$\phi_M(x_i, Q) = d_F^{-1}(Q) \int d^2k_\perp \theta(k_\perp^2 < Q^2) \psi_{q\bar{q}/M}(x_i, \vec{k}_\perp)$$

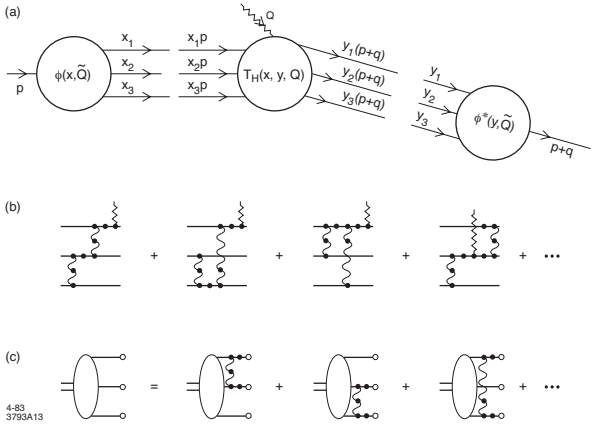

FIG. 11: (a) Factorization of the hard scattering amplitude applied to nucleon form factors at large momentum transfer. (b) The hard scattering amplitude T_H is computed at order α_s^2. (c) Leading order contributions to the evolution kernel for the nucleon distribution amplitude.

and

$$\phi_B(x_i, Q) = d_F^{-3/2}(Q) \int [d^2k_\perp] \theta(k_\perp^2 < Q^2) \psi_{qqq/B}(x_i, \vec{k}_\perp).$$

Here $d_F^{-1/2}$ is the renormalization factor for each fermion line. For simplicity, spin indices have been suppressed. The integration implies that the impact separation between the valence quarks is limited to $b_\perp^2 \leq 1/Q^2$. It is convenient to assume the light-cone gauge A^+0 so that the gluon fields have physical polarization; in gauges other than $A^+ = 0$ light-cone gauge, a Wilson line between the quark and antiquark fields is required. The distribution amplitudes $\phi(x_i, Q)$ are universal - they depend specifically on the valence LFWF of the hadron, and they are thus independent of the specific hard scattering process. The distribution amplitude is frame invariant, independent of the hadron's P_H^+ and $P_{\perp H}$. Since it is defined at fixed LF time, the distribution amplitude is also causal. One can also derive [62] the distribution amplitude $\phi_M(x_i, Q)$ from the hadron's Bethe-Salpeter wavefunction $< H|\overline{\psi}(x)\psi(0)|0 >$ evaluated at fixed LF time $\tau = x^+ = 0$..

The renormalization scale of $\alpha_s(\mu_R^2)$ appearing in T_H can be fixed at each order using the "Principle of Maximum Conformality (PMC)" [63], the rigorous extension of the BLM procedure [64]. One shifts the scale α_s so that none of the β_i terms associated with the evolution of the coupling appear. The resulting pQCD prediction is then scheme-independent and, to high accuracy, independent of the choice of the initial scale μ_R. The 'renormalon' terms which make the series diverge as $n!$ are absent. An important example is the pion form factor measured in $\ell\pi \to \ell\pi$. In this case the one gluon exchange kernel gives

$$F_\pi(Q^2) = \frac{16\pi\alpha_s(Q^2)}{3Q^2} \int_0^1 dx \int_0^1 dy \frac{\phi(x, \tilde{Q}_x)\phi(y\tilde{Q}_y)}{x(1-x)y(1-y)}$$

See Fig. 12. An approximate formula for meson form factors was first given by Farrar and Jackson in ref. [65]

At high transverse momentum, the meson LFWF falls off as $\psi_M(x, \vec{k}_\perp) \sim \alpha_s(k_\perp^2)/k_\perp^2$. The distribution amplitude thus evolves as the scale Q^2 of the hard subprocess increases. The resulting 'ERBL' [16, 17] evolution equation at

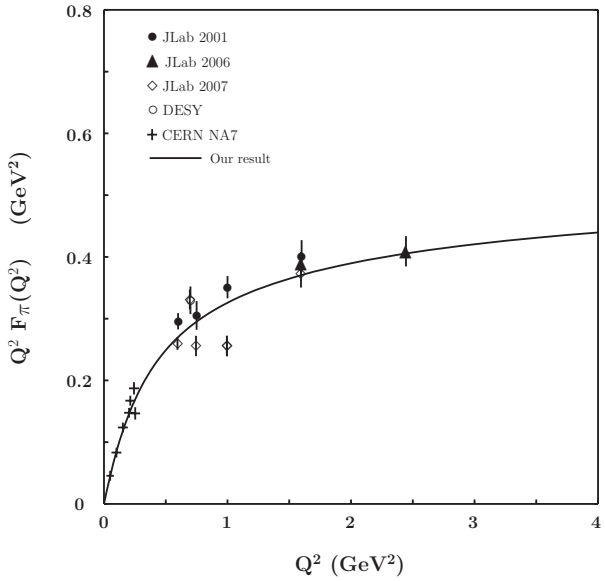

FIG. 12: The pion form factor compared with AdS/QCD predictions and pQCD. From ref. [66] The asymptotic power $Q^2 F_\pi(Q^2) \simeq$ constant is consistent with quark counting.

leading order in α_s is

$$Q\frac{\partial}{\partial Q}\phi(x,Q) = \frac{\alpha_s(Q^2)}{4\pi}\int_0^1 dy \frac{V(x,y)}{y(1-y)}[\phi(y,Q) - 2\phi(x,Q)]$$

The evolution kernel $V(x,y)$ is derived at leading order in pQCD from the one-gluon exchange interaction:

$$V(x,y) = 4C_F[x(1-y)\theta(y-x)\delta_{-h,\bar{h}} + \frac{\Delta}{y-x} + (x \to 1-x, y \to 1-y)] = V(y,x).$$

The operator Δ in the potential is defined such that

$$\Delta\frac{\phi(y,Q)}{y(1-y)} \equiv \frac{\phi(y,Q)}{y(1-y)} - \frac{\phi(x,Q)}{x(1-x)}$$

which eliminates the singular behavior at $y = x$.

Solutions of the ERBL evolution equation for the distribution amplitude has the general form

$$\phi(x,Q) = x(1-x)\sum_{n=0}^{\infty}\log[Q^2/\Lambda^2]^{-\gamma_n} a_n C_n^{3/2}(2x-1)$$

where the γ_n are the non-singlet anomalous dimensions associated with the operator product $\psi(z/2)\overline{\psi}(-z/2)$ where $z^+ = 0$:

$$\gamma_n = 2C_F[1 + 4\sum_{k=2}^{n+1}\frac{1}{k} - \frac{2\delta_{-(h,\bar{h})}}{(n+1)(n+2)}] \geq 0.$$

This expansion can also be obtained explicitly from the operator-product expansion near the light-cone; i.e., for $z^2 = -z_\perp^2 \sim 1/Q^2$. There is a corresponding evolution equation for the three-quark baryon distribution amplitude.

The coefficients a_n of the Gegenbauer polynomials $C_n^{3/2}$ that appear in the solution to the ERBL equation are determined from the nonperturbative dynamics of the meson; i.e., the form of $\phi_M(x, Q_0)$ at the nonperturbative QCD scale. The Q-independent coefficient a_0 can be determined from the decay meson constant f_M obtained from weak leptonic decays $u\bar{d} \to W^+ \to \bar{\mu}^+\nu$ since the anomalous dimension γ_0 vanishes: $\gamma_0 = 0$. For example, $a_0/6 = \int dx_0^1 \phi_\pi(x.Q) = f_\pi/2\sqrt{n}_C$. The large Q^2 behavior of the meson distribution amplitude at large Q^2 is universal: $\phi_M(x, Q \to \infty)x(1-x)f_\pi$, independent of the nonperturbative input. The underlying hadron LF wavefunction must vanish at $x, (1-x) \to 0$ to ensure that the expectation value of the LF kinetic energy $(k_\perp^2 + m^2)/x(1-x)$ is finite.

The LFWFs and their resulting distribution amplitudes can also be used to compute other hadronic observables; for example, the structure functions measured in deep inelastic scattering are effectively the probability distributions defined from the absolute squares of the LFWFs integrated over the transverse momenta [41]. The generalized parton amplitudes, such as E and H, which underly deeply virtual Compton scatting $\gamma * p \to \gamma p$ in the 'handbag' approximation, can also be evaluated as convolutions of initial and final proton LFWFs. An example is given in ref [67].

VI. LIGHT-FRONT HOLOGRAPHY

One of the most exciting recent developments in the analysis of exclusive processes in QCD has been a new approach to nonperturbative QCD based on 'light-front holography' [68]. Holography can relate a theory in five dimensions to a theory in one less dimension. The LF holographic analysis utilizes the compact AdS_5 space in 4+1 space-time dimensions, since it provides a geometrical representation of the conformal group and the invariant transverse separation $\vec{\zeta}_\perp^2 \equiv \frac{x}{1-x}\vec{\eta}_\perp^2$ in 3+1 space at fixed LF time τ is holographically dual [69] to the fifth dimension z coordinate in AdS_5 space. If one includes a factor of $\exp + \kappa^2 z^2$ (the 'dilaton') in the AdS_5 action, a confinement potential with a fundamental scale κ appears in the corresponding LF Schrödinger equations of motion in physical space time. See fig. 13 and ref. [68]

Remarkably, the resulting action in physical space-time remains conformal despite the appearance of the mass scale κ in the LF Hamiltonian and the equations of motion. The LF confinement potential in the meson sector has the unique harmonic oscillator form using the extension of principle of extended conformal invariance developed by de Alfaro, Fubini, Furlan [70] to LF theory. The resulting formalism is frame-independent and causal. Only one parameter, the mass scale that sets the scale of confinement $\kappa = \sqrt{\lambda}$ appears in the AdS/QCD analysis. One can solve the LF Schrödinger equation with the confining kernel $\kappa^4\zeta^2 = \kappa^4 b_\perp^2 x(1-x)$, derived from LF holography and AdS/QCD. The result is a pion with zero mass for $m_q = 0$ and pion excitations which satisfy the Regge form $M_{n,L}^2 = 2\kappa^2(n+L)$ with the same slope in n and L. this explaining important features of hadron dynamics [71]. The form of the nonperturbative distribution amplitude from this approach is is $\phi_\pi(x) = f_\pi\sqrt{x(1-x)}$ at small Q^2. See fig. 14. This form has also been recently derived using the Bethe-Salpeter formalism in ref. [72] The distribution then evolves by ERBL evolution to the universal asymptotic form, $\phi_\pi(x, Q) \to \frac{3f_\pi}{\sqrt{n_C}}x(1-x)$ at $Q^2 \to \infty$; i.e., the scale where all hadron structure functions evolve [73] by DGLAP evolution to δ functions at $x = 0$. For a recent review, see ref. [74] A corresponding LF Dirac equation resulting from light-front holography which determines nucleon spectroscopy and dynamics, can also be derived using superconformal quantum mechanics [75].

The hard scattering domain for hard exclusive processes is $z^2 = \vec{\zeta}_\perp^2 < x/(1-x)Q^2$, and thus the behavior of the AdS amplitude $\Phi(z)$ at small z controls exclusive amplitudes at large momentum transfer. Since the power-law behavior of $\Phi(z)$ at small z is determined by the twist of the short-distance interpolating operator of the hadron, the results agree with the quark counting rules, independent of the choice of the dilaton profile at large z, as was first shown for form factors by Polchinski and Strassler [18]. The LFWF for the ρ^0 meson obtained using same approach gives a remarkably good description of diffractive ρ electroproduction $\gamma * p \to \rho^0 p'$ as shown by Sandapen and Forshaw [77]. See fig.15. The meson distribution amplitudes play a central role in QCD phenomenology since they describe *hadronization at the amplitude level* – the transition between the off-shell quark and antiquark with momentum fractions x and $1-x$, transverse separation $b \perp \sim 1/Q$ and opposite helicities within the meson. Light-Front Holography also predicts the spectroscopy and dynamics [69, 78] for hadrons with half-integer spin from a Light-Front Dirac equation. One obtains

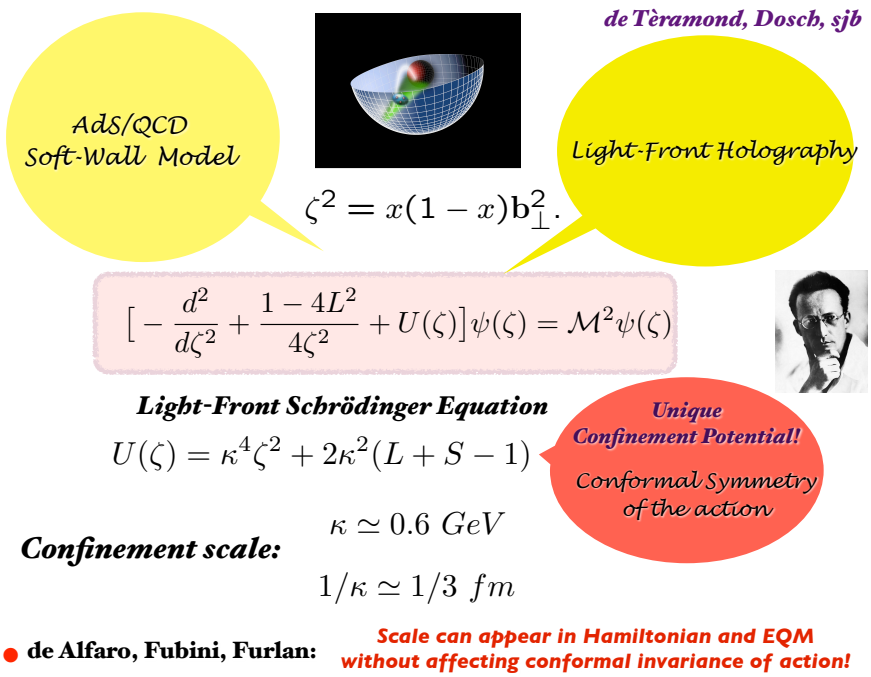

FIG. 13: The LF Schrödinger equation and LF wavefunction derived from AdS/QCD and LF holography. The unique form of the confinement potential $U(\zeta^2)$. is a consequence AdS/QCD and the principle of de Alfaro, Fubini, Furlan [70]. The eigenfunction LF Schrödinger equation predicts a zero-mass pion and the same Regge slope in n and L.

Regge trajectories with the same slope in n and L, thus reproducing the nucleon entries listed but the PDG. The same results can be also derived using superconformal algebra [75]. This formalism thus leads to dynamical predictions as well as spectroscopy. Predictions for the proton and neutron form factors from the AdS/QCD LF Dirac equation are shown in fig. 16.

A. The Photon-to-Pion Transition Form Factor from AdS/QCD Light-Front Holography

A primary test of the pQCD formalism for hard exclusive reactions is the photon-to-pseudo-scalar meson transition form factor $F_{\gamma\to M}(Q^2)$ since it only involves one hadron. It can be measured at e^+e^- colliders via two-photon reactions where one of the incident leptons scatters with large momentum transfer. and the other photon is nearly real: $k^2 \sim 0$. The invariant amplitude for the photon-to-pseudo-scalar meson transition form factor is defined as [16] $M_{\mu,\nu} = \epsilon_{\mu\nu\sigma\tau}p_M^\sigma q^\tau F_{\gamma\to M}(Q^2)$. The transition form factor can be computed from first principles at leading twist and leading order in α_s:

$$Q^2F_{\gamma\to M}(Q^2) = \frac{4}{\sqrt{3}}\int_0^1 dx \frac{\phi(x,(1-x)Q)}{1-x}[1+\mathcal{O}(\alpha_s,\frac{m^2}{Q^2})]$$

Since $\phi(x, Q\to\infty) = \sqrt{s}f_\pi x(1-x)$, the asymptotic photon-to-pion form factor is predicted without ambiguity: $Q^2F_{\pi\gamma}(Q^2\to\infty) = 2f_\pi$. A complete prediction [80, 81] valid at all Q^2 can be made using light-front holography including modifications from the dressed current derived from AdS_5. The AdS/QCD prediction is compared with measurements in fig. 17. The result is also consistent with the pQCD analysis, The Belle data [82] agrees well with the unified AdS/QCD predictions. However, the BaBar data [83] appears to diverge at $Q^2 \sim 10\ GeV^2$. A possibility is that the BaBar [83] signal, which deviates from the pQCD asymptotic prediction, includes a background contribution to $e^+e^-\to e^{+\prime}e^{-\prime}\pi^0$ events, due to the interference of contributions from the spacelike $\gamma^*\gamma\to\pi^0$ and timelike $\gamma^*\to\pi^0+\gamma$ transition form factors.

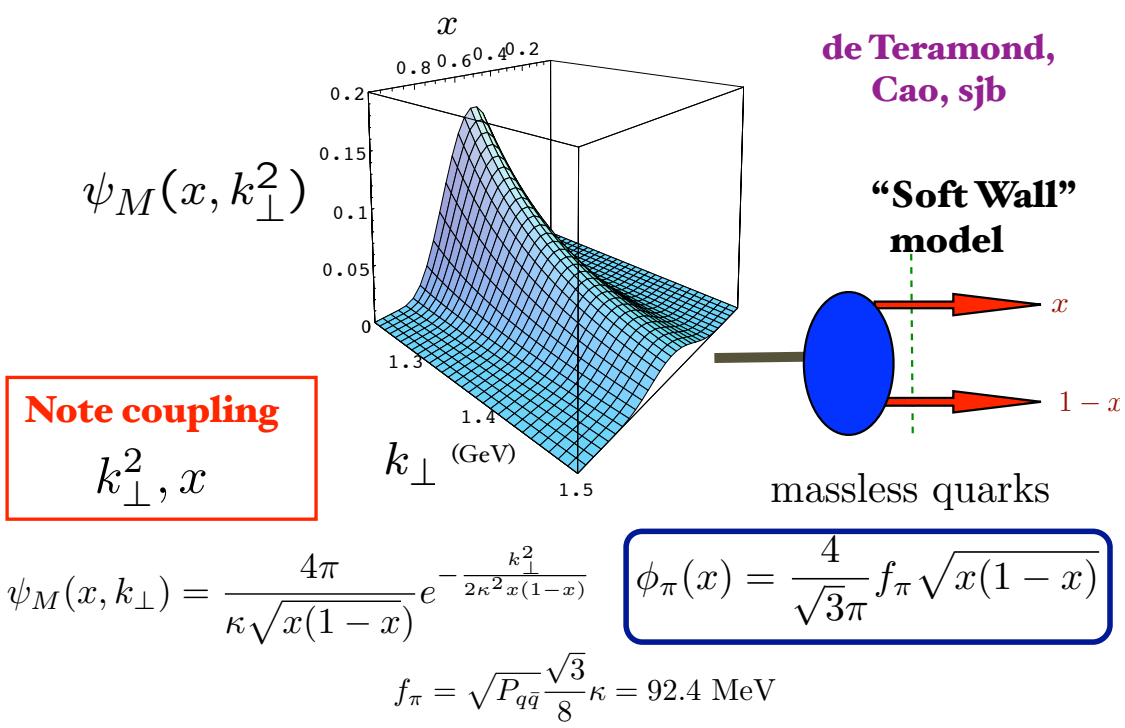

FIG. 14: Predictions for the pion LF wavefunction and distribution amplitude from the LF Schrodinger Equation [76].

B. Prediction for the QCD Running Coupling from AdS/QCD Light-Front Holography

Light-Front Holography also predicts the functional dependence of the QCD running coupling $\alpha_s(Q^2) \propto \exp -Q^2/4\kappa^2$ in the nonperturbative region of small Q^2 When one matches the running coupling $\alpha_s^{g1}(Q^2)$ defined from the Bjorken sum rule [87] and its derivative to the pQCD high Q^2 prediction using the $\overline{MS}$ scheme, one obtains a running coupling valid from low to high Q^2. See refs. [85, 86]. The value of $\Lambda_{\overline{MS}}$ can then be determined from the ρ mass. See fig. 18. The coupling $\alpha_s^{g1}(Q^2)$ is the effective charge defined from the Bjorken sum rule [88]. The AdS/QCD Light-Front Holography approach thus describes both the dynamics of exclusive process and the hadron spectrum in terms of one parameter, the mass scale κ. and a unique confining potential.

VII. CONCLUSIONS

The discovery of Bjorken scaling [89] in deep inelastic lepton-proton scattering [90, 91] – and its parton model interpretation by Feynman [92] and by Bjorken and Paschos [93] – was the critical observation showing that hadrons are indeed bound states of quarks. The discovery [94] of the scaling of $R_{e^+e^-}(s)$ and its stepwise character as one passes quark thresholds, counts the number of quark flavors that exist in nature. A third crucial discovery was that the fall-off of the rate for hard hadronic exclusive reactions, such as form factors at large momentum transfer, enumerates [1–3] the number of quarks or antiquarks in any hadronic bound state – two for mesons, three for baryons, six for the deuteron, etc. Thus even though quarks are confined and cannot emerge separately as asymptotic states, one use the scaling of exclusive amplitudes to rigorously count their degree of compositeness. We have also noted that by duality and the exclusive-inclusive connection, one obtains spectator counting rules [13] for the power-law fall-off of both structure functions at $x \to 1$ and fragmentation functions at $z \to 1$, predictions consistent with the Gribov-Lipatov crossing relations [95].

The quark counting rules apply not only to elastic and transition form factors, but also to hard exclusive $2 \to N$

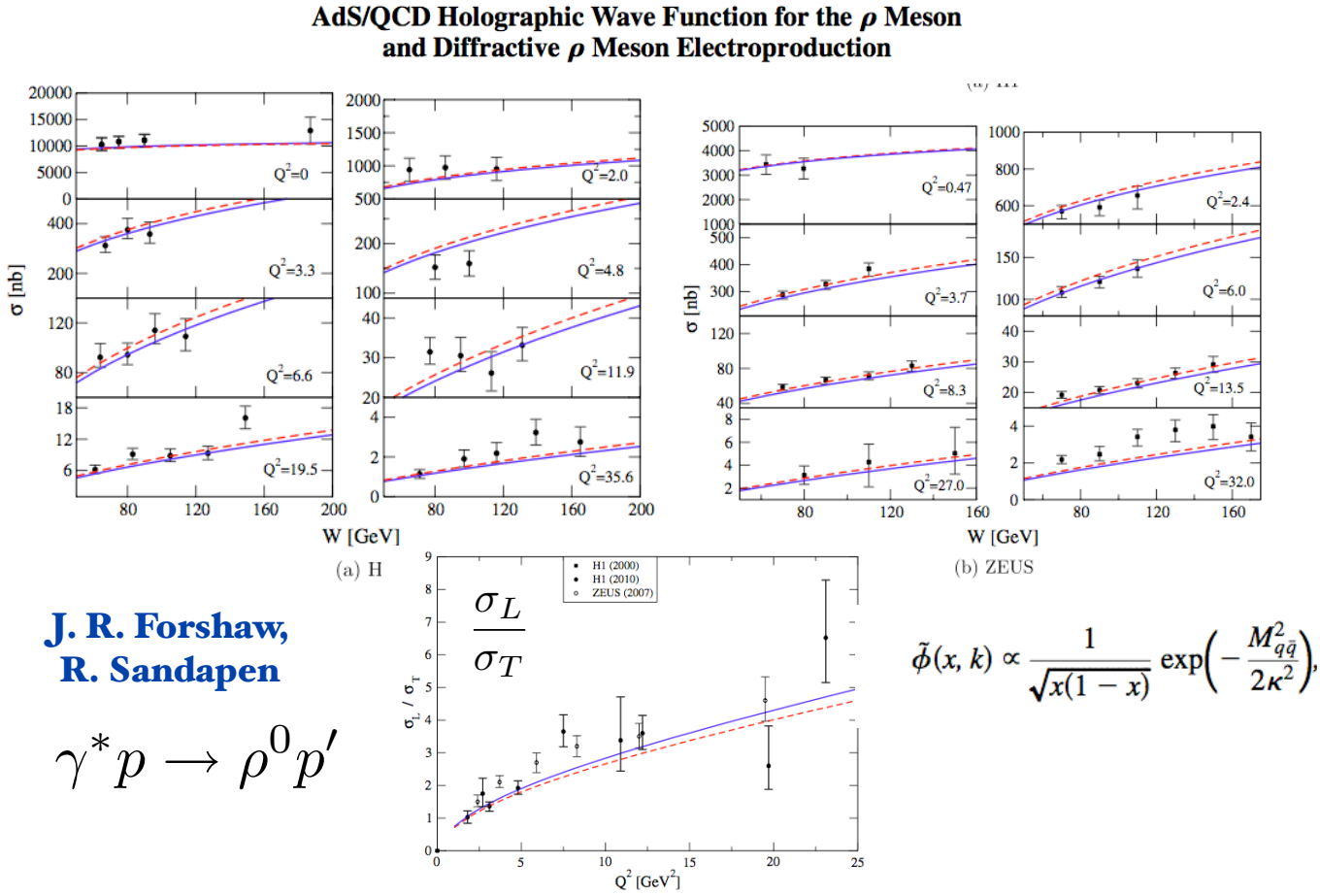

FIG. 15: Prediction [77] for diffractive ρ electroproduction $\gamma * p \to \rho^0 p'$ using the LFWF given by AdS/QCD and LF holography. There are no new parameters.

processes at fixed angle. The power-law fall-off reflects the twist of the leading interpolating operator for each hadron at short distances $x^2 \to 0$. The pQCD analysis give the leading power-law fall-off; one obtains corrections higher order in $1/Q^2$ and $1/p_T^2$ from higher non-valence Fock states, internal transverse momentum and mass scales. In addition, the pQCD analysis modifies the nominal leading power-law fall-off by anomalous dimensions derived from the operator product expansion, ERBL evolution of the distribution amplitudes [16, 17], and by the evolution of the QCD running coupling [96–98]. The counting rules can also be derived nonperturbatively [18] using light-front holography and the soft-wall modification of the AdS_5 action.

Constituent counting rules also provide an important tool for determining the structure of exotic hadrons [99]. For example, one could measure the power-law fall-off of the rate for the production of pairs of *tetraquarks* such as the Z_c^+ at large center of mass squared s:

$$\frac{\sigma(e^+e^- \to Z_c^+(c\bar{c}u\bar{d}) + \bar{Z}_{\bar{c}}^-(\bar{c}c\bar{u}d))}{\sigma(e^+e^- \to \mu\bar{\mu})} = |F_{Z_c}(s)|^2 \propto \frac{1}{s^N}$$

If $N = 2(4-1) = 6$, this would prove that the Z_c^+ is indeed a bound state of a two quarks and two antiquarks. One can also determine the constituent content of the Z_c^+ with a significantly larger rate by checking

$$\frac{\sigma(e^+e^- \to Z_c^+(c\bar{c}u\bar{d}) + \pi^-(\bar{u}d))}{\sigma(e^+e^- \to \mu\bar{\mu})} \propto \frac{1}{s^4}$$

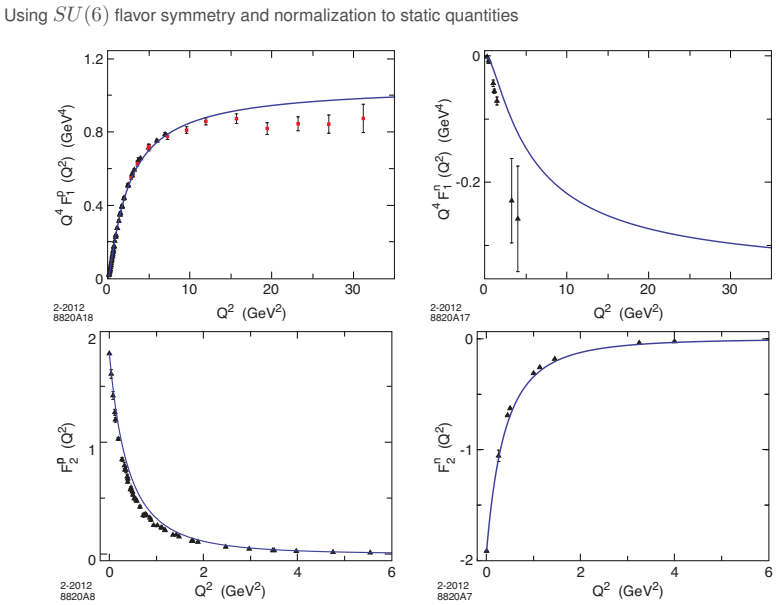

FIG. 16: Light-front holographic predictions [79] for the nucleon form factors normalized to their static values.

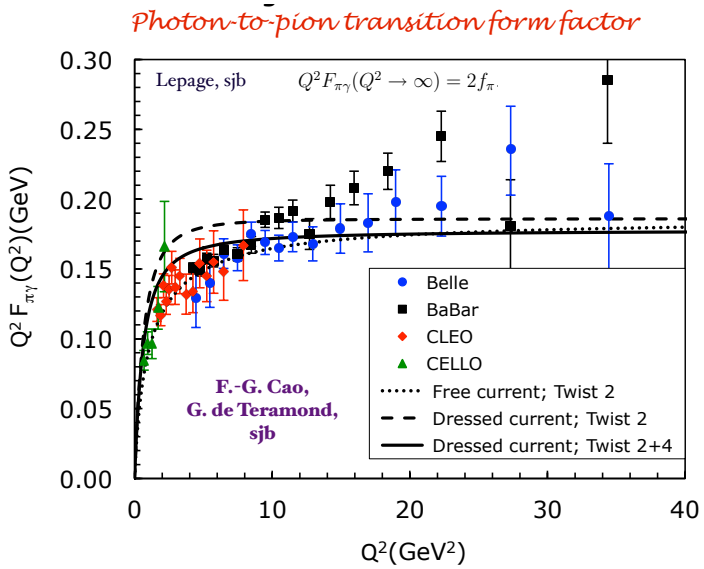

FIG. 17: The $\gamma\gamma^* \to \pi^0$ transition form factor: $Q^2 F_{\pi\gamma}(Q^2)$ as a function of $Q^2 = -q^2$. The dotted curve is the result predicted by AdS/QCD using a Chern-Simons form [80, 81] The dashed and solid curves include the effects of using a confined EM current for twist-2 and twist-2 plus twist-4, respectively. The high Q^2 data are from BaBar, ref. [83] and Belle, ref. [84]

since $N = 4 + 2 - 2 = 4$. The ratio of e^+e^- exclusive annihilation rates:

$$\frac{\sigma(e^+e^- \to Z_c^+(c\bar{c}u\bar{d}) + \pi^-(\bar{u}d))}{\sigma(e^+e^- \to \Lambda_c(cud)\bar{\Lambda}_c(\bar{c}\bar{u}\bar{d}))}$$

has cancelling heavy-quark mass and scaling corrections; its scaling should be sensitive to the fundamental QCD composition of the Z_c^+; e.g., whether it is primarily a "molecular" $([c\bar{c}] + [u\bar{d}])$ state, analogous to "nuclear-bound quarkonium" $(J/\psi + A)$ [100, 101], or whether it is a diquark-diquark $([c\bar{d}]_{3_C} + [u\bar{c}]_{3_C})$ resonance of QCD color-triplets [102].

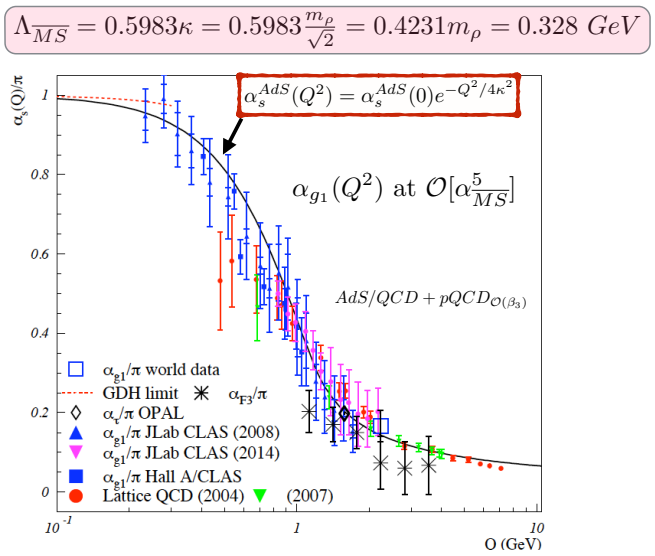

FIG. 18: Comparison of the analytical expression for α_{g_1} obtained by matching the hard pQCD and nonperturbative predictions from AdS/QCD and light-front holography with experimental JLab data for the Bjorken sum rule and, lattice QCD results. The coupling $\alpha_s^{g1}(Q^2)$ is the effective charge defined from the Bjorken sum rule. The constraint at $Q^2 = 0$ is derived from the Drell-Hearn Sum Rule. From ref. [85, 86].

Acknowledgments

This research was supported by the Department of Energy, contract DE–AC02–76SF00515. SLAC-PUB-16162. I am indebted to my collaborators who made these studies possible and to Professor Harald Fritzsch for his invitation to write this contribution to his historical volume, '50 Years of Quarks', to be published by World Scientific.

[1] S. J. Brodsky and G. R. Farrar, Phys. Rev. Lett. **31**, 1153 (1973).
[2] S. J. Brodsky and G. R. Farrar, Phys. Rev. D **11**, 1309 (1975).
[3] V. A. Matveev, R. M. Muradyan and A. N. Tavkhelidze, Lett. Nuovo Cim. **5S2**, 907 (1972) [Lett. Nuovo Cim. **5**, 907 (1972)].
[4] H. Fritzsch, M. Gell-Mann and H. Leutwyler, Phys. Lett. B **47**, 365 (1973).
[5] S. J. Brodsky, Y. Frishman and G. P. Lepage, Phys. Lett. B **167**, 347 (1986).
[6] S. J. Brodsky, P. Damgaard, Y. Frishman and G. P. Lepage, Phys. Rev. D **33**, 1881 (1986).
[7] S. J. Brodsky, Y. Frishman, G. P. Lepage and C. T. Sachrajda, Phys. Lett. B **91**, 239 (1980).
[8] X. d. Ji, J. P. Ma and F. Yuan, Phys. Rev. Lett. **90**, 241601 (2003) [hep-ph/0301141].
[9] P. V. Landshoff and J. C. Polkinghorne, Phys. Lett. B **44**, 293 (1973).
[10] D. W. Sivers, S. J. Brodsky and R. Blankenbecler, Phys. Rept. **23**, 1 (1976).
[11] S. J. Brodsky and G. P. Lepage, Adv. Ser. Direct. High Energy Phys. **5**, 93 (1989).
[12] S. D. Drell and T. M. Yan, Phys. Rev. Lett. **24**, 181 (1970).
[13] S. J. Brodsky, M. Burkardt and I. Schmidt, Nucl. Phys. B **441**, 197 (1995) [hep-ph/9401328].
[14] E. L. Berger and S. J. Brodsky, Phys. Rev. Lett. **42**, 940 (1979).
[15] G. P. Lepage and S. J. Brodsky, Phys. Rev. Lett. **43**, 545 (1979) [Erratum-ibid. **43**, 1625 (1979)].
[16] G. P. Lepage and S. J. Brodsky, Phys. Rev. D **22**, 2157 (1980).
[17] A. V. Efremov and A. V. Radyushkin, Phys. Lett. B **94**, 245 (1980).
[18] J. Polchinski and M. J. Strassler, Phys. Rev. Lett. **88**, 031601 (2002) [hep-th/0109174].
[19] S. J. Brodsky and G. P. Lepage, Phys. Rev. D **24**, 2848 (1981).
[20] S. J. Brodsky and M. Karliner, Phys. Rev. Lett. **78**, 4682 (1997) [hep-ph/9704379].
[21] S. Brodsky, G. de Teramond and M. Karliner, Ann. Rev. Nucl. Part. Sci. **62**, 1 (2012) [arXiv:1302.5684 [hep-ph]].
[22] S. J. Brodsky and A. H. Mueller, Phys. Lett. B **206**, 685 (1988).
[23] S. J. Brodsky, L. Frankfurt, J. F. Gunion, A. H. Mueller and M. Strikman, Phys. Rev. D **50**, 3134 (1994) [hep-ph/9402283].
[24] D. Dutta, K. Hafidi and M. Strikman, Prog. Part. Nucl. Phys. **69**, 1 (2013) [arXiv:1211.2826 [nucl-th]].
[25] D. Ashery, Prog. Part. Nucl. Phys. **56**, 279 (2006).
[26] R. J. Glauber and G. Matthiae, Nucl. Phys. B **21**, 135 (1970).
[27] R. H. Dalitz and D. R. Yennie, Phys. Rev. **105**, 1598 (1957).
[28] E. M. Aitala *et al.* [E791 Collaboration], Phys. Rev. Lett. **86**, 4773 (2001) [hep-ex/0010044].
[29] J. Aclander, J. Alster, G. Asryan, Y. Averiche, D. S. Barton, V. Baturin, N. Buktoyarova and G. Bunce *et al.*, Phys. Rev. C **70**, 015208 (2004) [nucl-ex/0405025].
[30] E. A. Crosbie, L. G. Ratner, P. F. Schultz, J. R. O'Fallon, D. G. Crabb, R. C. Fernow, P. H. Hansen and A. D. Krisch *et al.*, Phys. Rev. D **23**, 600 (1981).
[31] S. J. Brodsky and G. F. de Teramond, Phys. Rev. Lett. **60**, 1924 (1988).
[32] M. Bashkanov, S. J. Brodsky and H. Clement, Phys. Lett. B **727**, 438 (2013) [arXiv:1308.6404 [hep-ph]].
[33] J. F. Gunion, S. J. Brodsky and R. Blankenbecler, Phys. Rev. D **8**, 287 (1973).
[34] S. J. Brodsky and B. T. Chertok, Phys. Rev. Lett. **37**, 269 (1976).
[35] S. J. Brodsky and B. T. Chertok, Phys. Rev. D **14**, 3003 (1976).
[36] V. A. Matveev and P. Sorba, Nuovo Cim. A **45**, 257 (1978).
[37] V. A. Matveev and P. Sorba, Lett. Nuovo Cim. **20**, 435 (1977).
[38] S. J. Brodsky, C. R. Ji and G. P. Lepage, Phys. Rev. Lett. **51**, 83 (1983).
[39] B. L. G. Bakker and C. R. Ji, Prog. Part. Nucl. Phys. **74**, 1 (2014).
[40] P. A. M. Dirac, Rev. Mod. Phys. **21**, 392 (1949).
[41] S. J. Brodsky, H. C. Pauli and S. S. Pinsky, Phys. Rept. **301**, 299 (1998) [hep-ph/9705477].
[42] H. C. Pauli and S. J. Brodsky, Phys. Rev. D **32**, 2001 (1985).
[43] S. S. Chabysheva and J. R. Hiller, arXiv:1409.6333 [hep-ph].
[44] B. L. G. Bakker, A. Bassetto, S. J. Brodsky, W. Broniowski, S. Dalley, T. Frederico, S. D. Glazek and J. R. Hiller *et al.*, Nucl. Phys. Proc. Suppl. **251-252**, 165 (2014) [arXiv:1309.6333 [hep-ph]].
[45] K. Hornbostel, S. J. Brodsky and H. C. Pauli, Phys. Rev. D **41**, 3814 (1990).
[46] S. Hellerman and J. Polchinski, In *Shifman, M.A. (ed.): The many faces of the superworld* 142-155 [hep-th/9908202].
[47] S. J. Brodsky, G. F. de Tramond and H. G. Dosch, Few Body Syst. **55**, 407 (2014) [arXiv:1310.8648 [hep-ph]].
[48] G. B. West, Phys. Rev. Lett. **24**, 1206 (1970).
[49] S. J. Brodsky and S. D. Drell, Phys. Rev. D **22**, 2236 (1980).
[50] R. Alkofer, A. Holl, M. Kloker, A. Krassnigg and C. D. Roberts, Few Body Syst. **37**, 1 (2005) [nucl-th/0412046].
[51] S. J. Brodsky, In *Brandeis Univ 1969, Proceedings, Atomic Physics and Astrophysics, Vol.1*, New York 1971, 91-169
[52] S. J. Brodsky and J. R. Primack, Annals Phys. **52**, 315 (1969).
[53] S. Weinberg, Phys. Rev. **150**, 1313 (1966).
[54] J. B. Kogut and D. E. Soper, Phys. Rev. D **1**, 2901 (1970).
[55] D. E. Soper, Phys. Rev. D **15**, 1141 (1977).
[56] H. T. C. Stoof, J. M. V. A. Koelman and B. J. Verhaar, Phys. Rev. B **38**, 4688 (1988).
[57] C. White, R. Appel, D. S. Barton, G. Bunce, A. S. Carroll, H. Courant, G. Fang and S. Gushue *et al.*, Phys. Rev. D **49**,

58 (1994).
[58] P. V. Landshoff, Phys. Rev. D **10**, 1024 (1974).
[59] S. Wallon, arXiv:1403.3110 [hep-ph].
[60] N. Isgur and J. E. Paton, Phys. Rev. D **31**, 2910 (1985).
[61] G. P. Lepage and S. J. Brodsky, Phys. Lett. B **87**, 359 (1979).
[62] J. Segovia, L. Chang, I. C. Clot, C. D. Roberts, S. M. Schmidt and H. s. Zong, Phys. Lett. B **731**, 13 (2014) [arXiv:1311.1390 [nucl-th]].
[63] S. J. Brodsky, M. Mojaza and X. G. Wu, Phys. Rev. D **89**, 014027 (2014) [arXiv:1304.4631 [hep-ph]].
[64] S. J. Brodsky, G. P. Lepage and P. B. Mackenzie, Phys. Rev. D **28**, 228 (1983).
[65] G. R. Farrar and D. R. Jackson, Phys. Rev. Lett. **43**, 246 (1979).
[66] T. Gutsche, V. E. Lyubovitskij, I. Schmidt and A. Vega, arXiv:1410.6424 [hep-ph].
[67] S. J. Brodsky, M. Diehl and D. S. Hwang, Nucl. Phys. B **596**, 99 (2001) [hep-ph/0009254].
[68] G. F. de Teramond and S. J. Brodsky, Phys. Rev. Lett. **102**, 081601 (2009) [arXiv:0809.4899 [hep-ph]].
[69] S. J. Brodsky and G. F. de Teramond, Phys. Rev. Lett. **96**, 201601 (2006) [hep-ph/0602252].
[70] V. de Alfaro, S. Fubini and G. Furlan, Nuovo Cim. A **34**, 569 (1976).
[71] S. J. Brodsky, G. F. De Tramond and H. G. Dosch, Phys. Lett. B **729**, 3 (2014) [arXiv:1302.4105 [hep-th]].
[72] L. Chang, I. C. Cloet, J. J. Cobos-Martinez, C. D. Roberts, S. M. Schmidt and P. C. Tandy, Phys. Rev. Lett. **110**, no. 13, 132001 (2013) [arXiv:1301.0324 [nucl-th]].
[73] C. G. Callan, Jr. and D. J. Gross, Phys. Rev. Lett. **22**, 156 (1969).
[74] S. J. Brodsky, G. F. de Teramond, H. G. Dosch and J. Erlich, arXiv:1407.8131 [hep-ph].
[75] G. F. de Teramond, H. G. Dosch and S. J. Brodsky, arXiv:1411.5243 [hep-ph].
[76] S. J. Brodsky and G. de Teramond, Int. J. Mod. Phys. Conf. Ser. **20**, 53 (2012) [arXiv:1208.3020 [hep-ph]].
[77] J. R. Forshaw and R. Sandapen, Phys. Rev. Lett. **109**, 081601 (2012) [arXiv:1203.6088 [hep-ph]].
[78] G. F. de Tramond, S. J. Brodsky and H. G. Dosch, EPJ Web Conf. **73**, 01014 (2014) [arXiv:1401.5531 [hep-ph]].
[79] G. F. de Teramond and S. J. Brodsky, arXiv:1203.4025 [hep-ph].
[80] S. J. Brodsky, F. G. Cao and G. F. de Teramond, Phys. Rev. D **84**, 075012 (2011) [arXiv:1105.3999 [hep-ph]].
[81] S. J. Brodsky, F. G. Cao and G. F. de Teramond, Phys. Rev. D **84**, 033001 (2011) [arXiv:1104.3364 [hep-ph]].
[82] S. Uehara *et al.* [Belle Collaboration], Phys. Rev. D **86**, 092007 (2012) [arXiv:1205.3249 [hep-ex]].
[83] B. Aubert *et al.* [BaBar Collaboration], Phys. Rev. D **80**, 052002 (2009) [arXiv:0905.4778 [hep-ex]].
[84] H. Nakazawa [Belle Collaboration], PoS ICHEP **2012**, 356 (2013).
[85] S. J. Brodsky, G. F. de Tramond, A. Deur and H. G. Dosch, arXiv:1410.0425 [hep-ph].
[86] A. Deur, S. J. Brodsky and G. F. de Teramond, arXiv:1409.5488 [hep-ph].
[87] J. D. Bjorken, Phys. Rev. D **1**, 1376 (1970).
[88] S. J. Brodsky, G. F. de Teramond and A. Deur, Phys. Rev. D **81**, 096010 (2010) [arXiv:1002.3948 [hep-ph]].
[89] J. D. Bjorken, Phys. Rev. **148**, 1467 (1966).
[90] E. D. Bloom, D. H. Coward, H. C. DeStaebler, J. Drees, G. Miller, L. W. Mo, R. E. Taylor and M. Breidenbach *et al.*, Phys. Rev. Lett. **23**, 930 (1969).
[91] M. Breidenbach, J. I. Friedman, H. W. Kendall, E. D. Bloom, D. H. Coward, H. C. DeStaebler, J. Drees and L. W. Mo *et al.*, Phys. Rev. Lett. **23**, 935 (1969).
[92] R. P. Feynman, In *Brown, L.M. (ed.): Selected papers of Richard Feynman* 560-655
[93] J. D. Bjorken and E. A. Paschos, Phys. Rev. **185**, 1975 (1969).
[94] B. Richter, Conf. Proc. C **751125**, 327 (1975).
[95] V. N. Gribov and L. N. Lipatov, Sov. J. Nucl. Phys. **15**, 438 (1972) [Yad. Fiz. **15**, 781 (1972)].
[96] H. D. Politzer, Phys. Rept. **14**, 129 (1974).
[97] D. J. Gross and F. Wilczek, Phys. Rev. D **9**, 980 (1974).
[98] A. J. Buras, Rev. Mod. Phys. **52**, 199 (1980).
[99] H. Kawamura, S. Kumano and T. Sekihara, arXiv:1410.0494 [hep-ph].
[100] S. J. Brodsky, I. A. Schmidt and G. F. de Teramond, Phys. Rev. Lett. **64**, 1011 (1990).
[101] M. E. Luke, A. V. Manohar and M. J. Savage, Phys. Lett. B **288**, 355 (1992) [hep-ph/9204219].
[102] S. J. Brodsky, D. S. Hwang and R. F. Lebed, Phys. Rev. Lett. **113**, 112001 (2014) [arXiv:1406.7281 [hep-ph]].